Magneto-Optical Spectrum Analyzer

M. Helsen,[1, a)] A. Gangwar,[2] A. Vansteenkiste,[1] and B. Van Waeyenberge[1]
[1)] *Department Solid State Sciences, Ghent University, Krijgslaan 281/S1, 9000 Ghent, Belgium*
[2)] *Department of Physics, Universität Regensburg, Universitätsstrasse 31, 93040 Regensburg, Germany*

(Dated: 27 May 2014)

We present a method for the investigation of gigahertz magnetization dynamics of single magnetic nano elements. By combining a frequency domain approach with a micro focus Kerr effect detection, a high sensitivity to magnetization dynamics with submicron spatial resolution is achieved. It allows spectra of single nanostructures to be recorded. Results on the uniform precession in soft magnetic platelets are presented.

arXiv:1405.6551v1 [physics.ins-det] 26 May 2014

I. INTRODUCTION

Magnetism at the sub-micrometer and nano scale attracts a great deal of interest for both fundamental reasons and for their prospective use in logic and memory applications. As not only the static properties, such as the magnetic magnetic domain configuration, but also the dynamics properties on the sub-nanosecond timescale (e.g. the resonances and magnetization switching) are strongly determined by the reduced dimensionality, appropriate characterization techniques are required. The conventional method for high frequency characterisation of magnetic systems is the cavity based ferromagnetic resonace technique. However, nanostuctures can not be studied in remanence as the fixed frequency operation requires the bias field to be swept. To address this problem, different techniques have been developed. Dependent on how the magnetic response is detected they can be divided in two categories. Vector Network Analyzer Ferromagnetic Resonance (VNA-FMR[3,4]) and Pulsed Inductive Microwave Magnetometry (PIMM[5,6]) detect the resonance electrically and in Time Resolved Magneto-Optical Kerr Effect (TR-MOKE[7]) and Time Resolved Scanning Transmission X-Ray Microscopy experiments (STXM[8–10]) optical detection is used. The optical methods have a high sensisitivity to detect the signal of a single magnetic microstructure, but have a much more complicated set-up than the electrical methods, and require a femtosecond laser or pulsed X-ray source. On the other hand, detection in the frequency domain, like conventional FMR and VNA-FMR can achieve much higher signal-to-noise ratios[3]. Here we present an approach which combines the frequency domain method with optical detection: the Magneto-Optical Spectrum Analyzer (MOSA).

This method is a hybrid method between VNA-FMR and TR-MOKE in the context of measurement abilities and construction. TR-MOKE makes use of a pulsed laser to probe the magnetization ($\vec{M}$) through the magneto-optical Kerr effect[11–15] at regular intervals, while the sample is excited using e.g. another laser pulse or a microwave signal generator. By shifting the arrival time of the probe pulses with respect to the excitation, time domain information can be gathered. This method, on the other hand probes the magnetization using a continuous wave laser and measures (again through the Kerr effect) the fast change of magnetization with an ultrafast photodiode in the frequency domain.

II. DESCRIPTION OF THE SET-UP

Shown in Fig.1 is the optical layout of our set-up. Light (660nm) from a laser diode (LD) is linearly polarized using a polarizer (Pol) and passes through a non-polarizing beamsplitter (BS). An objective lens (L1) focusses it to a diffraction limited spot ($\approx$ 500nm) on the sample, where microwave interconnects provide RF current for the excitation and an electromagnet can provide a bias field of up to 50mT.

The reflected light is collected by the same objective lens and redirected by the beamsplitter onto an analyzer (An). The tranmission axis of this analyzer is set at an angle of 45° with respect to the transmission axis of the first polarizer. The beam is then focussed using an aspheric lens (L2) onto a multimode optical fiber (MM Fiber), transporting it over a large distance (50 m in our case) to an ultrafast photodiode (PD) with a bandwidth of approximately 12GHz. At this point intensity variations are measured.

The objective lens is mounted on a piezo stage to allow scanning of the probe beam over the sample surface. By recording the DC reflected light intensity, we can image the sample and correctly focus and position the probe beam on the sample. For this purpose the light is deflected with a mirror towards a conventional photodiode (both not shown for clarity).

The out-of-plane magnetization dynamics are measured via the polar Kerr effect. When reflecting off the sample, linearly polarized lights gains both an ellipticity (ϵ_K) and a rotation of the major polarization axis, known as the Kerr angle (θ_K). For out-of-plane saturated Permalloy, the polar Kerr angle is typically 1 mrad[16]. Both the sign and magnitude of this angle depend on the sign and magnitude of the out-of-plane magnetization of

[a)] Electronic mail: Mathias.Helsen@UGent.be

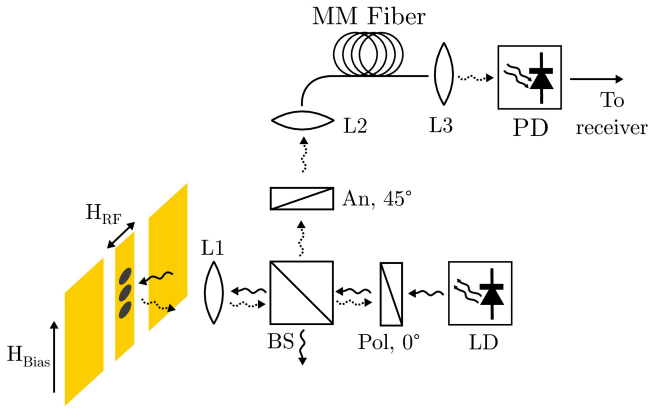

FIG. 1. A basic sketch of the optical part of the set-up, used for polar Kerr detection. LD is a laser diode, Pol a polarizer, BS a non-polarizing beamsplitter, L1 an objective lens, An an analyzer, L2 and L3 aspheric lenses and PD an ultrafast photodiode. The angle between the transmission axis of Pol and An is 45°.

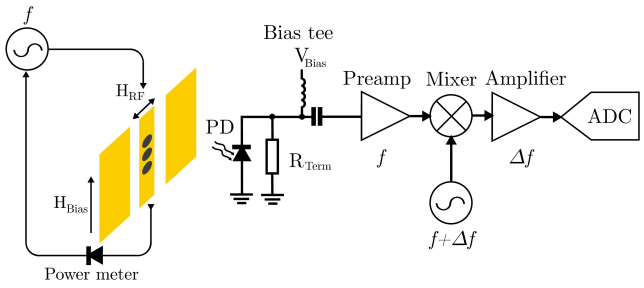

FIG. 2. A simplified schematic of the electrical part of the set-up. A diode detector connected to the sample helps in keeping the power transmitted through the sample level when the frequency is varied. Also shown are the photodiode (PD), termination resistor (R_{Term}), bias tee, RF preamplifier, frequency mixer, low frequency amplifier and ADC. Both signal generators produce a tone in the microwave range (f), but are slightly offset by frequency Δf in the kHz range.

the probed area.

The reflected light is analyzed with the polarizer at an angle of 45°, thus yielding an intensity of $I = I_0(1/2 + \theta_{\mathrm{K}})$, where I_0 is the intensity before the analyzer. Placing the analyzer at 45° maximizes the signal.

The electrical part of the set-up is shown in Fig. 2. One signal generator produces the RF current at frequency f used for exciting the sample. The RF power through the sample is kept level by using a diode detector measuring the power coming out of the sample. The bias tee provides the necessary bias voltage and shunts the DC photocurrent. The DC photocurrent flowing out of the bias tee is measured for monitoring purposes.

Assuming a linear dependence of the light intensity on the magnetization[11,14], we can estimate the AC current induced in the photodiode due to magnetization dynamics as $\delta I \approx I_{\mathrm{DC}}\theta_{\mathrm{K,max}}\delta m_z$, where $\theta_{\mathrm{K,max}}$ is the Kerr angle at saturation ($M_z = M_{\mathrm{S}}$), δm the reduced out-of-plane magnetization (M_z/M_{S}) and I_{DC} the DC photocurrent.

The AC photocurrent is passed on to the low noise preamplifier, which increases the signal level by 30dB. After this preamplifier, a mixer downconverts this high frequency signal to a frequency in the audio range. To this end a second signal generator, phase locked to the first one, produces a high frequency signal at a frequency offseted by several kilohertz (Δf) with respect to the excitation frequency f. Thus, the signal that the mixer produces is at the frequency Δf. It is further amplified by a second amplifier and finally sampled using a high end ADC. A computer records the incoming data from the ADC and performs an FFT to compute the signal strength at Δf.

III. COMPARISON WITH OTHER METHODS

To estimate the detection limit of the set-up, we compare the typical signal levels to the fundamental noise present. There are three main contributions to this noise[17]:

- a contribution from the DC photocurrent, known as shot noise, with a current noise density given by $i_{\mathrm{noise}} = \sqrt{2qI_{\mathrm{DC}}}$;
- a contribution from the noise intrinsic to the diode, quantified by the Noise Equivalent Power (NEP);
- and a contribution from the terminating resistor, R_{Term} (50Ω), known as Johnson noise, with a voltage noise density given by $v_{\mathrm{noise}} = \sqrt{4kTR_{\mathrm{Term}}}$.

We assume that these are sources of white noise and that all other possible sources generate much less noise in the frequency range of interest.

If we compare this noise with the signal strength, we arrive at the following expression for the Signal-to-Noise Ratio (SNR) at the input of the preamp:

$$\mathrm{SNR} = 10\log_{10}\frac{I_{\mathrm{DC}}^2\theta_{\mathrm{K}}^2\langle m_z^2\rangle}{B(2qI_{\mathrm{DC}} + 4kT/R_{\mathrm{Term}} + (\mathcal{R}\cdot\mathrm{NEP})^2)}, \tag{1}$$

where B is the measurement bandwidth and $\mathcal{R}$ the responsivity of the photodiode (A/W (at a specific wavelength)). Typical values for our set-up would involve $I_{\mathrm{DC}} = 100.0\mu$A, $B = 1$Hz and $\langle m_z^2\rangle = 10^{-4}$. The Johnson noise is the largest contribution ($1.8\cdot10^{-11}$ A/$\sqrt{\mathrm{Hz}}$), followed by the shot noise ($5.7\cdot10^{-12}$ A/$\sqrt{\mathrm{Hz}}$). In comparision, the NEP for the photodiode we have used is negligible (only $4.5\cdot10^{-17}$ A/$\sqrt{\mathrm{Hz}}$). Because the contribution from shot noise is still smaller than the Johnson

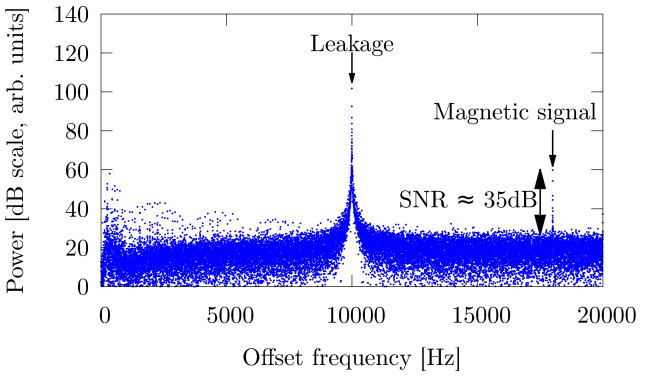

FIG. 3. Shown is a FFT when both a magnetic signal and a direct coupling are present. In this particular case a Permalloy disc with a diameter of 20μm was excited at 4GHz with +10dBm of power and biased with a field of 20mT. The leakage was caused by a microstrip, which was properly terminated and carried the same amount of power as used for the excitation, but at a slightly different frequency.

noise, the SNR can be significantly improved by increasing the light intensity incident on the photodiode. Only when the photocurrent reaches 1 mA (equivalent to 10 mW optical power on the diode) does the shot noise exceed the Johnson noise. However increasing light intensity also entails heating up to sample, even to above the Curie temperature. A further increase in SNR could be obtained by cooling the detector, lowering the Johnson noise.

Adding these terms we find a SNR of approximatly 34dB. In addition, the first amplifier adds a noise figure of 2dB, thus the final SNR is about 32dB. But as the signal itself is on the order of -130dBm or $5 \cdot 10^{-14}$ mW, absolute care in handling the microwave signals is still required.

To illustrate this, we have excited a sample with enough RF power (+10dBm) so that the it would precess with $\delta m_z \approx 0.01$. The same amount of RF power but at a slightly offseted frequency was sent through a microstrip next to the receiver, to allow for a comparison between the magnetic signal and the direct coupling from the excitation to the receiver. The result in Fig. 3 shows that direct coupling is much stronger than the magnetic signal and that our estimate of the SNR is quite accurate. To this end, the detection has been separated by a large distance from the excitation. Low frequency $1/f$ noise is not showing due to a low frequency cut-off characteristic of the low frequency amplifier, but the noise floor increases below 5kHz.

Our method is complementary to both VNA-FMR and TR-MOKE. To the former, we add the advantage of spatial selectivity. This means that several magnetic structures can be fabricated in each others vicinity and we are still able to probe each one separately, or that the spatial variation of the magnetization dynamics can be analyzed, in contrast to VNA-FMR.

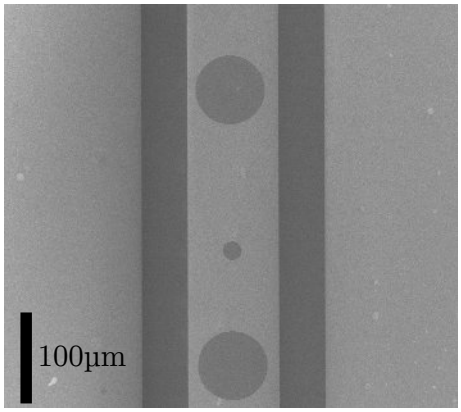

FIG. 4. A SEM micrograph of a sample used for measurements. The dots are 75μm and 20μm in diameter.

Where TR-MOKE is a time domain method, we are measuring directly in frequency domain, thus it is easier to measure resonance curves directly and not have to rely on Fourier transforms of time domain data. In comparison to pulsed methods, we have independent control of frequency and amplitude, resulting in non-ambiguous spectra. Further, our method allows us to probe the signal at any arbitrary frequency, something that is difficult to do with stroboscopic time domain measurement methods.

One last advantage of our method is that it does not require a femtosecond pulsed laser, high end oscilloscope or vector network analyzer, thus eliminating a large cost.

IV. EXPERIMENTAL DETAILS

As an illustration we have measured the uniform precession of magnetization in Permalloy discs with a 20μm diameter. The samples were fabricated on a silicon substrate. Structure definitions were made with electron beam lithography and the lift-off technique. After the last metal deposition an ALD coating of Al_2O_3 was deposited. The samples were then wire bonded to a high frequency substrate. An example of such a sample is shown in Fig. 4.

An example of a resonance curve where the frequency is swept at a fixed field of 45mT, is shown in Fig. 5. The peak was fitted to a Lorentz curve and the resulting resonance frequency was determined to be 6120±2 MHz, with a linewidth of 188±4 MHz. This illustrates that the linewidth can be accuratly measured on single microscopic elements.

The detector itself has a frequency dependence, making the recorded spectrum a product of the magnetic response and the detector response. To investigate this effect, a frequency sweep was performed for a different number of bias fields and the resonance frequency was determined for each. In Fig. 6 the resulting datapoints are compared with the Kittel equa-

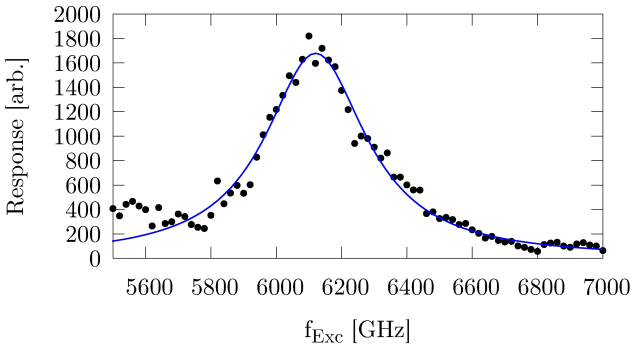

FIG. 5. The resonance curve for a 20μm diameter, 50nm thickness Permalloy disc in a field of 45mT. The solid line is the Lorentzian fit.

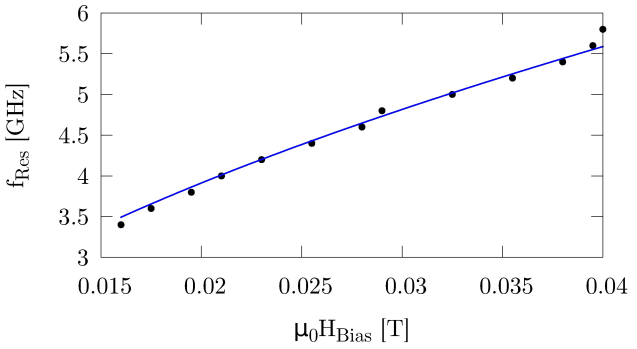

FIG. 6. The evolution of the resonance peak of the uniform precession when the field is increased. The Kittel equation for a thin film is shown as a black line.

tion, which for an infinitly thin film is given by $f_{\mathrm{Res}} = 28.0\sqrt{\mu_0 H_{\mathrm{Bias}}(\mu_0 H_{\mathrm{Bias}} + \mu_0 M_s)}$ GHz/T. Literature values have been used for calculating the Kittel equation ($\mu_0 M_s = 1.04$T)[18]. The datapoints are in good agreement with the Kittel equation, ruling out strong frequency variations in the detection which might interfere with measurements.

Finally, the magnetic signal can also be used for imaging purposes; when the laser beam is scanned over the sample using the piezo stage and the magnetic signal at each point is recorded. This can be compared with the reflectivity, which is acquired simultaneously. When the sample is excited at resonance, the contrast is highest. An example is shown in Fig. 7. Here we compare the reflectivity (clearly showing the Au CPW, Si substrate and Permalloy discs) with the magnetic signal showing only the Permalloy disc.

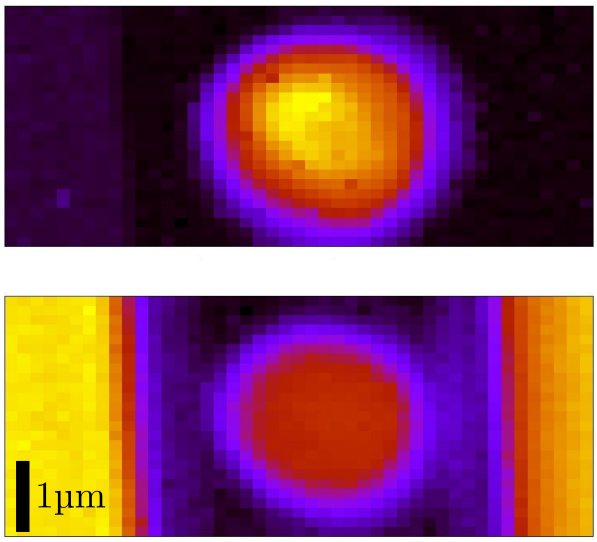

FIG. 7. At the top an image generated using the magnetic response of a uniform resonance in a 3μm dot at 6GHz. Shown at the bottom is an image generated using reflectivity data that was collected simultaneously.

V. CONCLUSION

We have developed a method of probing magnetization dynamics at the multiple-GHz range using a frequency domain method that offers spatial sensitivity. The set-up is relatively simple, yet allows for high quality measurements, thus enabling a fast exploration of excitation parameters. We have illustrated that our method can yield quantitative results using uniform excitation on single microscopic elements.

ACKNOWLEDGMENTS

Mathias Helsen, Arne Vansteenkiste and Bartel Van Waeyenberge acknowledge funding by FWO-Vlaanderen and BOF-UGent.

1

2 "-1."

3 I. Neudecker, G. Woltersdorf, B. Heinrich, T. Okuno, G. Gubbiotti, and C. Back, "Comparison of frequency, field, and time domain ferromagnetic resonance methods," *J. Magn. Magn. Mater.*, vol. 307, p. 148, 2006.

4 S. Kalarickal, P. Krivosik, M. Wu, C. Patton, M. Schneider, P. Kabos, T. Silva, and J. Nibarger, "Ferromagnetic resonance linewidth in metallic thin films: Comparison of measurement methods," *J. Appl. Phys.*, vol. 99, p. 093909, 2006.

5 A. Kos, T. Silva, and P. Kabos, "Pulsed inductive microwave magnetometer," *Rev. Sci. Instrum.*, vol. 73, p. 3563, 2002.

6 T. Silva, C. Lee, T. Crawford, and C. Rogers, "Inductive measurement of ultrafast magnetization dynamics in thin-film permalloy," *J. Appl. Phys.*, vol. 85, p. 7849, 1999.

7 Y. Acremann, M. Buess, C. Back, M. Dumm, G. Bayreuther, and D. Pescia, "Ultrafast generation of magnetic fields in a Schottky diode," *Nature*, vol. 414, p. 51, 2001.

[8]M. Bolte, G. Meier, B. Krüger, A. Drews, R. Eiselt, L. Bocklage, S. Bohlens, T. Tyliszczak, A. Vansteenkiste, B. Van Waeyenberge, K. W. Chou, A. Puzic, and H. Stoll, "Time-resolved x-ray microscopy of spin-torque-induced magnetic vortex gyration," *Phys. Rev. Lett.*, vol. 100, p. 176601, Apr 2008.

[9]A. Vansteenkiste, K. W. Chou, M. Weigand, M. Curcic, V. Sackmann, H. Stoll, T. Tyliszczak, G. Woltersdorf, C. H. Back, G. Schutz, and B. Van Waeyenberge, "X-ray imaging of the dynamic magnetic vortex core deformation," *Nat Phys*, vol. 5, pp. 332–334, May 2009.

[10]M. Kammerer, M. Weigand, M. Curcic, M. Noske, M. Sproll, A. Vansteenkiste, B. Van Waeyenberge, H. Stoll, G. Woltersdorf, C. H. Back, and G. Schuetz, "Magnetic vortex core reversal by excitation of spin waves," *Nat Commun*, vol. 2, pp. 279–, Apr. 2011.

[11]P. N. Argyres, "Theory of the Faraday and Kerr Effects in Ferromagnetics," *Phys. Rev.*, vol. 97, no. 2, pp. 334–345, 1955.

[12]J. Zak, E. Moog, C. Liu, and S. Bader, "Universal approach to magneto-optics," *J. Magn. Magn. Mater.*, vol. 89, p. 107, 1990.

[13]S. Polisetty, J. Scheffler, S. Sahoo, Y. Wang, T. Mukherjee, X. He, and C. Binek, "Optimization of magneto-optical kerr setup: Analyzing experimental assemblies using Jones matrix formalism," *Rev. Sci. Instrum.*, vol. 79, p. 055107, 2008.

[14]A. Zvezdin and V. Kotov, *Modern Magnetooptics and Mangetooptic Materials*. Institute of Physics Publishing, 1997.

[15]Z. Qiu and S. Bader, "Surface magneto-optic Kerr effect," *Rev. Sci. Instrum.*, vol. 71, no. 3, p. 1243, 2000.

[16]M. Veis and R. Antos, "Advances in Optical and Magnetooptical Scatterometry of Periodically Ordered Nanostructured Arrays," *J. Of Nanomaterials*, 2012.

[17]P. Horowitz and W. Hill, *The art of electronics*. Cambridge University Press, 1989.

[18]J. Coey, *Magnetism and Magnetic Materials*. Cambridge University Press, 2010.